URTeC: 2670158

The Use of Time-Lapse Seismic Attributes for Characterizing Hydraulic Fractures in a Tight Siltstone Reservoir

Riazi*, N., Clarkson, C.R., University of Calgary

 DOI 10.15530/urtec-2017-2670158

This paper was prepared for presentation at the Unconventional Resources Technology Conference held in Austin, Texas, USA, 24-26 July 2017.

Summary

With the use of multi-fractured horizontal wells (MFHWs) now commonplace for the development of low-permeability (tight) and shale reservoirs, a premium has been placed on hydraulic fracture characterization methodologies that can be used to improve development efficiency. There are now multiple techniques that can be used to characterize hydraulic fractures during and after the stimulation treatment. Time-lapse seismic offers advantages over more conventionally-used microseismic because surveys can be collected before, during, and after stimulation treatment, providing the opportunity to observe reservoir system changes during the treatment. Further, seismic surveys can be more carefully designed because they don't rely on passive signals from the reservoir. Finally, time-lapse seismic can be used to evaluate reservoir system changes in three dimensions and at larger scales than microseismic.

In this study, the impact of hydraulic fractures generated during stimulation treatment of two MFHWs on time-lapse seismic data is evaluated. The target reservoir is a low-permeability siltstone in the Montney Formation, western Canada. The objectives of this study are several-fold: 1) to analyze time-lapse multi-component seismic data collected during stimulation treatment in order assess the orientation and spatial position of hydraulic fractures; 2) to analyze compressional and shear velocity changes in the reservoir due to hydraulic fractures by performing time-lapse seismic inversion; 3) to compare different time-lapse seismic attributes to determine which ones are most consistent with independent fracture characterization methods, and 4) to evaluate the effect of flowback on seismic data.

This study demonstrates that time-lapse seismic attributes can be used to evaluate induced fracture location and orientation in the study area. It is further illustrated that PS seismic data are effective for characterizing the fractured regions due to the incorporation of shear wave (S) data along with compressional wave (P) data. Shear wave splitting maps provided partially consistent results with those of microseismic and other methods used to characterize the hydraulic fractures. Importantly, modeling performed herein demonstrates how velocities vary during flowback. The results of this study have important implications for the characterization of fractured zones in tight reservoirs.

Introduction

Low permeability ('tight') and shale reservoirs have been considered important targets of exploration and development in North American industry in recent years. Multi-fractured horizontal wells (MFHWs) play a key role in the development of tight/shale reservoirs, leading to commercial production. Therefore, characterization of MFHWs using different methods is of importance to operators to improve well performance (Clarkson et al. 2016). While many operators choose to develop these plays using a "pattern" drilling and completion strategy, tight reservoirs exhibit significant complexity and heterogeneity that can lead to sub-optimal and inefficient development.

Petrophysical and geophysical methods can help to better characterize tight reservoir heterogeneity, which in turn can be used in more efficient development. Clarkson et al. (2012a) discussed some of the challenges of tight reservoir characterization using multiple techniques, while Clarkson et al. (2016) emphasized the need for characterization of shale gas reservoirs at multiple scales. Those authors did not focus on the use of seismic data for characterizing tight reservoirs. More relevant to the current study, Riazi et al. (2017) illustrated the use of ultrasonic measurements for characterizing sub-core-scale heterogeneity in tight rock core plugs by evaluating elastic anisotropy and shear wave splitting results as a function of effective pressure.

Seismic data can provide valuable information about vertical and horizontal changes in reservoir characteristics, which is particularly useful in reservoirs with high heterogeneity and complexity. For example, Riazi and Clarkson (2016) and Mirzayev et al. (2017) demonstrated how seismic attributes aided in the detection of fractures in the tight middle Bakken reservoir of Viewfield, Saskatchewan, with the latter study demonstrating how this information can be used in connectivity analyses.

While 3D seismic analysis is useful for characterizing reservoir/fracture properties at the time that the survey is shot, time-lapse seismic analyses, such as time-lapse seismic inversion, can provide valuable information about dynamic changes in the reservoir that occur during recovery processes (e.g. Lumley 2001, Riazi et al. 2015). Specific to tight reservoirs, it is desirable to use time-lapse seismic analysis to evaluate hydraulic fracture properties (by comparison of results before and after hydraulic fracturing) and the impact of early time production on the dynamic properties of the reservoir. The intent of the current study is therefore to apply time-lapse seismic analysis, with a focus on seismic inversion, to a tight gas reservoir in western Canada.

In the following, a brief overview of the study area and the data available is first provided. Next, the theory and methods used for the study are discussed, including rock physics modeling, time-lapse seismic inversion, and PS seismic analysis. Finally, the results of these methods applied to the studied reservoir are provided, as well as a discussion of which seismic attributes were most helpful in characterizing post-stimulation reservoir/fracture properties. This study should be of interest to those geophysicists and petroleum engineers performing field-scale reservoir and hydraulic-fracture characterization studies in tight reservoirs.

Study Area and Previous Work

The study area is located in the southern portion of the Pouce Coupe pool in Alberta, Canada. The reservoir targets studied in this work are low-permeability siltstones within the Middle Triassic Montney Formation that were developed first with hydraulically-fractured vertical wells, and then later with MFHWs. The geologic setting of the Montney is discussed comprehensively in other works (e.g. Edwards et al. 1994). The finely-laminated siltstones have been subdivided into multiple units, two of which (Unit C and Unit D) are the tight reservoir intervals studied herein and elsewhere (e.g. Atkinson 2010). A type log is provided in **Fig. 1**. These laminated siltstones mostly exhibit micro-darcy-level permeability, as determined from detailed core analysis (Clarkson et al. 2012b), with few, if any natural fractures, observed in core.

Numerous reservoir characterization studies have been performed at the study location, including detailed core analysis studies (Clarkson et al. 2012a,b), microseismic and time-lapse seismic studies (e.g. Atkinson 2010, Steinhoff 2013, and Duenas 2014), and rate-transient analysis of the producing vertical wells and MFHWs (Clarkson and Beierle 2011). The focus of the current study is on time-lapse seismic analysis in this study area. This study differs from previous work on time-lapse seismic in the area, such as that by Duenas (2014) where seismic inversion was only performed on the base seismic survey (Phase 1). The current work provides additional results, such as seismic attributes associated with time-lapse seismic data. This work is also different from that of Steinhoff (2013) because differences in shear wave splitting characteristics over all surveys were compared in the current work, rather than providing just the individual shear wave splitting maps as in the Steinhoff work. This comparison helps to emphasize elastic property changes occurring in the reservoir due to the hydraulic fracturing and flowback processes.

Dataset Used for Current Study

A comprehensive dataset containing PP (P-wave) and PS (converted wave) time-lapse seismic data, along with microseismic data, and well log data, were available for analysis in the study area. Three multicomponent seismic surveys were acquired by Talisman Energy in December 2008 to monitor the hydraulic-fracture stimulation activity in multi-fractured horizontal wells targeting both Unit C and Unit D within the Montney of the study area.

The first seismic survey was acquired before hydraulic fracturing of the MFHWs in the study area, and the second and third after hydraulic fracturing two adjacent wells, well 2-07 and well 7-07, respectively (Fig. 1). The 7-07 well is completed in the Montney Unit D interval, and the 2-07 is completed in the Montney Unit C interval.

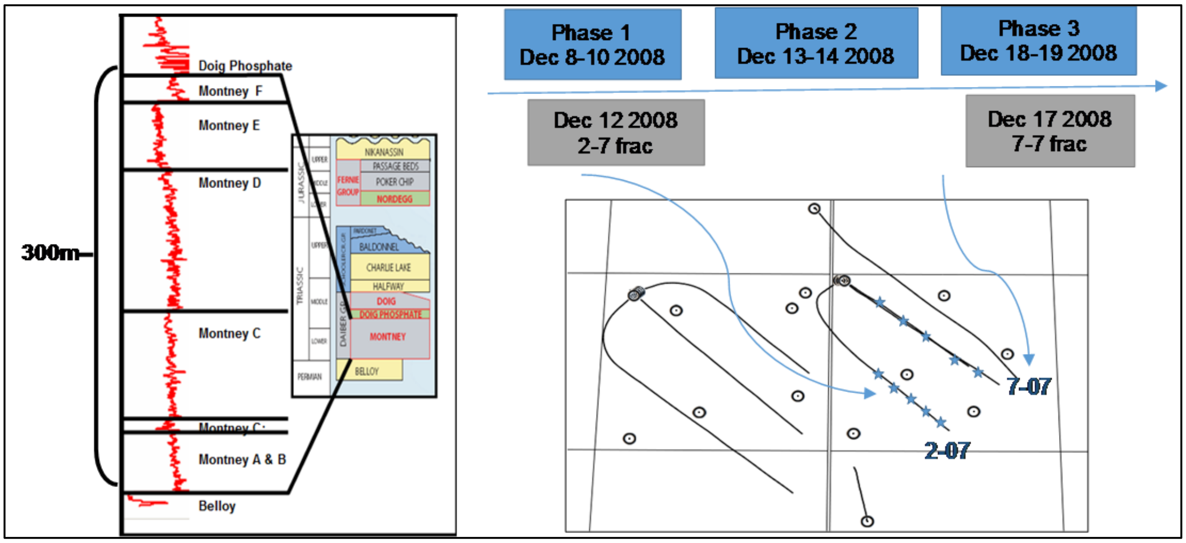

Fig. 1. (left) Type log of the Pouce Coupe Field - the red curve is the gamma ray log (modified from Steinhoff 2013). (right) Base map showing the location of two wells (2-07 and 7-07) monitored with time-lapse seismic. Also noted is the timing of hydraulic fracturing of the wells (grey boxes) and seismic surveys (three phases, blue boxes), which were acquired on three different dates in December 2008 (modified from Atkinson 2010).

Methodology

To characterize the Montney tight gas siltstone reservoir in the study area, different techniques were utilized to quantitatively evaluate variations in elastic properties in the reservoir due to hydraulic fracturing and during flowback of the two adjacent wells (2-07 and 7-07):

- Rock physics modeling
- Time-lapse seismic inversion
- PS seismic analyses

Rock Physics Modeling. Rock physics modeling was performed to better understand the changes observed in the time-lapse seismic data. Gassmann substitutional modeling was used to derive the elastic moduli due to saturation and pressure changes. The Gassmann equations (Gassmann 1951) are very commonly used and are a standard technique for seismic fluid substitution. Gassmann (1951) estimated the effect of fluid saturation changes on the elastic parameters in the reservoir. In his equations, bulk modulus of saturated rock can be estimated by using the dry bulk modulus and fluid and rock properties. The basic relationship for initial P-wave and S-wave velocity can be expressed using Equation 1:

$$K_{sat} = K_{dry} + \frac{\left(1 - \frac{K_{dry}}{K_m}\right)^2}{\frac{\phi}{K_{fl}} + \frac{1-\phi}{K_m} - \frac{K_{dry}}{{K_m}^2}} \quad (1)$$

$$G_{sat} = G_{dry} \quad (2)$$

where Ø is porosity, K_{dry} is the bulk modulus of the dry porous frame of the rock, K_{fl} is the bulk modulus of the fluid and K_m is the bulk modulus of the mineral. G_{sat} and G_{dry} are shear modulus of saturated rock and dry rock, respectively. The assumptions in this equation are that the pore space is interconnected and the pore pressure is in equilibrium. The fluid modulus is given by the weighted harmonic average of the bulk moduli of the individual phases as shown with Equation 3:

$$\frac{1}{K_{fl}} = \frac{S_w}{K_w} + \frac{S_o}{K_o} + \frac{S_g}{K_g} \quad (3)$$

where S_w, S_o and S_g are the water, oil and gas saturations, respectively, and K_w, K_o and K_g are the water, oil and gas moduli, respectively. In the Gassmann equations (Gassmann 1951), the shear modulus is constant for varying saturation at constant porosity, because the shear modulus is unaffected by the pore fluid (fluid cannot transmit shear waves). Saturated P-wave and S-wave velocities can be estimated using Equations 4 and 5 (the Gassmann equations):

$$V_{P-sat} = \sqrt{\frac{K_{sat} + \frac{4}{3}G_{sat}}{\rho_{sat}}} \tag{4}$$

$$V_{S-sat} = \sqrt{\frac{G_{sat}}{\rho_{sat}}} \tag{5}$$

where V_{P_sat} and V_{S_sat} are the saturated P-wave and S-wave velocities, respectively. The density ρ_{sat} is found using the volume average equation given by Equation 6:

$$\rho_{sat} = \rho_m(1-\phi) + \rho_w S_w \phi + \rho_o S_o \phi + \rho_g S_g \phi \tag{6}$$

To understand the effect of pressure on elastic properties of tight reservoirs, Gassmann modeling can also be used; in this case relationships between K_{dry} and porosity and effective pressure are employed. The pressure function used in this modeling approach for the study area is estimated using the laboratory-measured velocities versus effective pressure from Riazi et al. (2017). Although the pressure function was derived for the Montney reservoir by Riazi et al., the core samples were obtained from a different geographic location and depth, with likely differences in lithology. Some error is therefore expected in the current modeling if the samples are not representative of the study area. The porosity relationship with effective pressure is derived from available core analyses in the adjacent well.

After deriving the compressional and shear velocities with effective pressure, K_{eff} and μ_{eff} can be calculated and then substituted in the Gassmann equation to account for both pressure and saturation effects.

Time-lapse Seismic Inversion. Reservoir characterization involves the integration of different disciplines such as geology, geophysics, and engineering. To be able to integrate geophysical results with engineering inputs, quantitative seismic methods such as inversion are valuable. Seismic inversion is a technique to quantitatively analyze reservoir anomalies, and can provide both a static and dynamic description of the reservoir. By implementing seismic inversion, the link between reservoir engineering inputs and seismic data can be quantified.

In inversion, an attempt is made to recover the reflectivity by removing the wavelet effect. If the reflectivity is recovered, the acoustic impedance (which is the product of P-wave velocity and density) can be derived from the equation below:

$$Z_{p_{i+1}} = Z_{p_i}\left(\frac{1+R_i}{1-R_i}\right) \tag{7}$$

where $Z_{p_i} = \rho_i V_{P_i}$ is the acoustic impedance at the ith interface. In the above model, the assumptions include no multiples and a vertical raypath.

The seismic inversion technique can be applied to time-lapse seismic data (called time-lapse seismic inversion). The purpose of this is to produce different elastic properties for the base and monitor seismic surveys. Time-lapse seismic inversion can be applied to both post-stack and pre-stack seismic data. If seismic inversion is performed on pre-stack seismic data, more information can be extracted, such as shear impedance and density information, in addition to acoustic impedance through seismic volumes.

The algorithm used for pre-stack inversion herein is the simultaneous seismic inversion technique introduced by Hampson et al. (2005). In simultaneous inversion, pre-stack seismic data are inverted to P-impedance, S-impedance, and density volumes simultaneously. Simultaneous seismic inversion solves the Fatti et al. (1984) equation, which is a modification of the Aki-Richards equation (Aki and Richards, 1980):

$$R_{PP}(\theta) \approx a\, R_P + b\;\; R_S + c\, R_D \tag{8}$$

where R_P, R_S, R_D are the P-, S- and Density reflectivities, respectively. The scale values *a*, *b*, and *c* are defined as:

$$a = \frac{1}{2} sec^2\theta \tag{9}$$

$$b = -4\left(\frac{V_S}{V_P}\right)^2 sin^2(\theta) \tag{10}$$

$$c = \frac{1}{2} - 2\left(\frac{V_S}{V_P}\right)^2 sin^2(\theta) \tag{11}$$

For a given $R_{PP}(\theta)$, the Fatti et al. (1994) equation can be derived as:

$$S_{PP}(\theta) = aW(\theta)DL_P + bW(\theta)DL_S + cW(\theta)DL_D \tag{12}$$

where *W(θ)* is the wavelet matrix, which is dependent on *θ* (angle of incidence), *D* is the derivative matrix, and *L* is the log of the impedance values defined below:

$$L_P = \ln(Z_P) \tag{13}$$

$$L_S = ln\,(Z_S) \tag{14}$$

$$L_D = ln\,(\rho) \tag{15}$$

where Z_s is shear impedance, which is the product of shear velocity and density. One of the important features of this pre-stack inversion approach is the relationship between P- and S-velocities and their background trend. For additional information on this pre-stack inversion technique, please refer to Hampson et al. (2005).

For performing pre-stack seismic inversion, an initial model needs be defined to provide the low frequency information and be utilized as an initial guess in the seismic inversion process. In addition to initial low frequency acoustic impedance, initial low frequency shear impedance and density volumes are also created during the pre-stack simultaneous inversion process.

Due to the availability of time-lapse seismic inversion, different seismic attributes such as Poisson's ratio and Lamé attributes can be extracted. Lamé attributes have been very useful for identifying geomechanical "sweet spots" and have been shown to be lithology-dependent (Goodway et al. 2010). The two parameters of interest, Lambda ("incompressibility") and Mu ("rigidity"), may be calculated as follows:

$$Lambda = \lambda = \rho({V_P}^2 - 2{V_S}^2) \tag{16}$$

$$Mu = \mu = \rho {V_S}^2 \tag{17}$$

Time-lapse PS Analyses. Shear wave splitting (SWS) is an important phenomenon caused by wave propagation through an anisotropic medium. Measurement of the difference between fast and slow shear wave velocities can provide significant information about heterogeneity and the presence of fractures in the reservoir. In microseismic analyses, shear wave splitting can be helpful for evaluating reservoir and hydraulic fracture properties (Teanby et al. 2004, Verdon and Kendall 2011). Riazi et al. (2017) illustrated how SWS decreases with an increase in effective pressure for core plug samples taken from the Montney reservoir (in a different study area to the one herein). SWS can also be estimated from time-lapse PS seismic data. In PS seismic analyses, the reflected S wave splits into two orthogonal fast and slow shear modes, which are called PS1 and PS2, respectively. SWS can be estimated from the difference in arrival times of fast and slow shear velocities (in PS1 and PS2 seismic volumes) from the Thomsen (1986) relationship for a transverse isotropic medium:

$$\gamma = \frac{c_{66} - c_{44}}{2c_{44}} \tag{18}$$

where c_{66} and c_{44} are elastic constants. Equation 18 can be written in terms of velocities as:

$$\gamma \approx \frac{V_{s2} - V_{s1}}{V_{s1}} \tag{19}$$

where V_{s2} and V_{s1} can be derived from PS1 and PS2 times:

$$\gamma \approx \frac{\Delta t_{PS2} - \Delta t_{PS1}}{\Delta t_{PS1}} \tag{20}$$

Results

Rock Physics Modeling. As noted in the previous section, rock physics modeling helps one to interpret time-lapse seismic data. Specifically, this modeling can be used to determine the impact of fluid saturations and pressures on seismic velocities. In this section, therefore, two scenarios are shown where saturation and effective pressure vary in the reservoir. The modeling was performed for a well in the study area where compressional and shear velocities exist. **Fig. 2** illustrates the changes observed in P-velocity, S-velocity and density logs caused by adding 10% percent more gas in the reservoir (noting that the initial gas saturation is 60%). However, because there was initially high gas saturation in the system, adding 10% more gas does not significantly affect the velocity values. The impact of effective pressure is greater – **Fig. 3** demonstrates that P-velocity increases significantly with increasing effective pressure. Grey or black bars in this figure correspond to greater changes in seismic velocities, whereas white areas correspond to smaller changes in the modeled well. In summary, the pressure effect has a stronger impact on seismic velocity than saturation changes for the case studied.

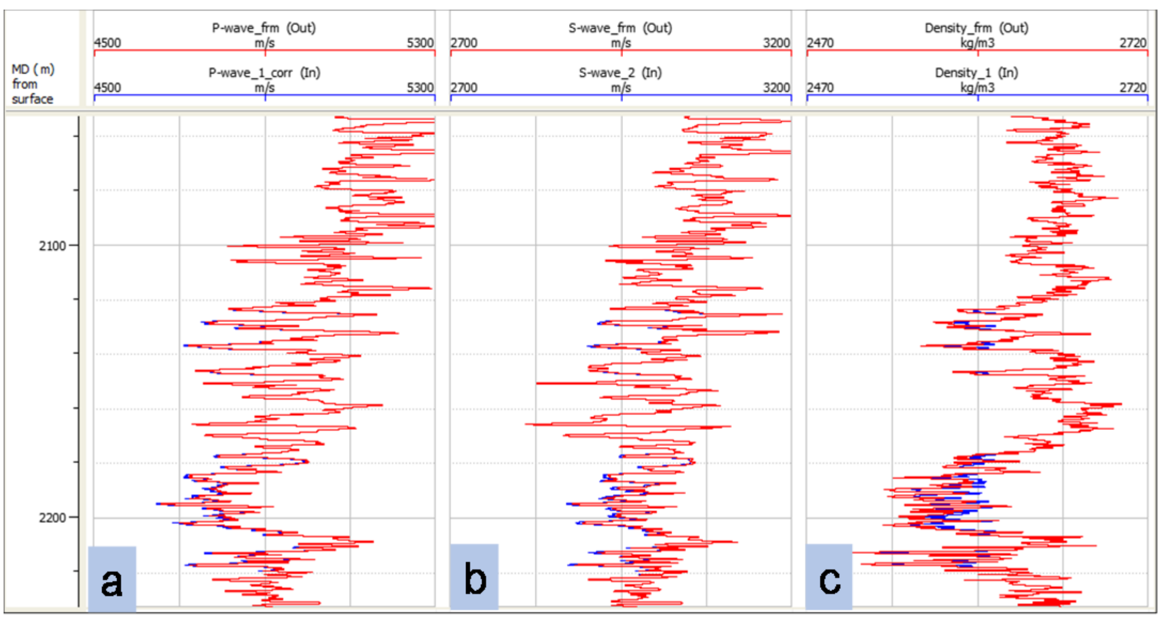

Fig. 2. Rock physics modeling results performed for a well in the study area. The (a) and (b), and (c) tracks illustrate changes in P-velocity, S-velocity, and density logs caused by adding 10 percent more gas to the reservoir. The blue lines represent these values prior to addition of gas, while the red lines are those after the addition. While P-velocity and density decrease and S-velocity increases, the amount of change is very small due to low porosity, and the presence of a high gas saturation initially in the reservoir.

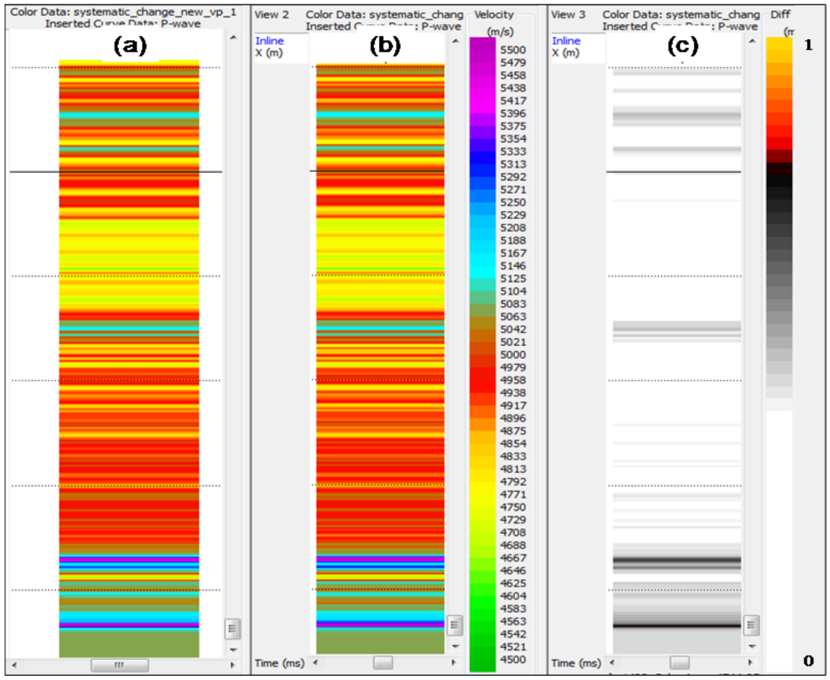

Fig. 3. The effect of effective pressure on P-velocity. P-velocity model for (a) 3MPa; (b) 6 MPa; and (c) the difference in P-velocity between (a) and (b) (color key in (c) is normalized). The darker colors in (c) illustrate greater differences in velocity. In summary, the pressure effect is stronger than that caused by saturation changes. The variation observed in this model is caused by porosity changes in the well.

Time-lapse Seismic Inversion. As discussed earlier, due to the availability of time-lapse pre-stack seismic data, pre-stack seismic inversion was performed. Pre-stack seismic inversion on time-lapse seismic data provided acoustic impedance, shear impedance, and density volumes for the three seismic surveys (before and after fracturing the two adjacent wells, Fig. 1). The low frequency initial model is an important input for inversion algorithm because it compensates for the lack of low frequency information in the seismic data and constrains the inversion. The low frequency acoustic impedance, shear impedance, and density initial models were derived by applying low-pass frequency filtering of the corresponding logs and integrating seismic horizons. **Fig. 4** illustrates a seismic section of the initial low frequency model and the result of seismic inversion for the base (Phase 1) seismic survey. This process was repeated for the two monitor surveys (Phase 2 and Phase 3, after hydraulic fracturing of 2-07 and 7-07, respectively) allowing changes in the reservoir caused by hydraulic fracturing and flowback to be evaluated. **Fig. 5** illustrates the difference between acoustic impedance and V_P/V_S ratio for the Phase 1 and Phase 3 surveys. V_p/V_s ratio volume was derived by the dividing the acoustic impedance by shear impedance. It can be seen that the acoustic impedance difference map in Unit D highlights more changes in the reservoir compared to the difference map in V_p/V_s. This is because acoustic impedance is sensitive to both effective pressure and fluid saturation changes whereas V_p/V_s is more affected by the fluid saturation changes in the reservoir. The V_p/V_s difference map (Unit D) highlights anomalies focused close to well 7-07, which was landed in Montney D.

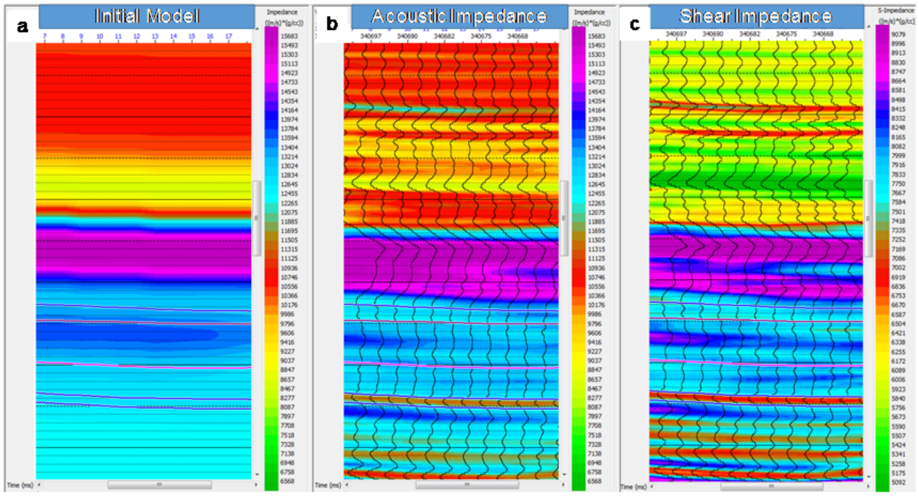

Fig. 4. Inversion results: a) initial low frequency model for acoustic impedance, b) acoustic impedance, and c) shear impedance results.

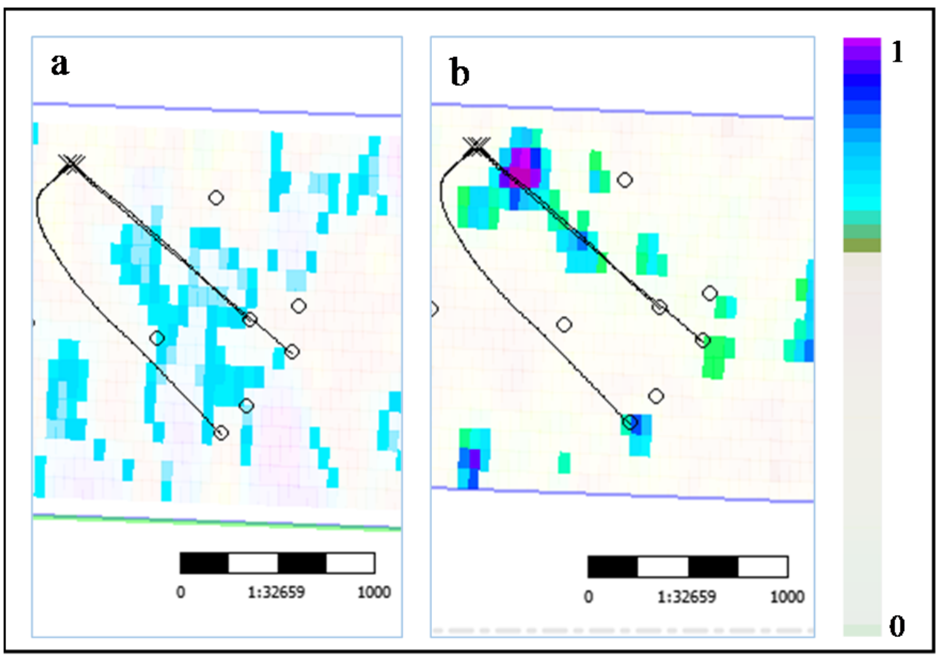

Fig. 5. The normalized average difference in a) acoustic impedance and b) V_p/V_s ratio for Montney Unit D. The difference between the surveys for Phase 1and Phase 3 are shown, the latter after hydraulically fracturing the 7-07 well.

Time-lapse PS Analyses. The intent of the PS seismic analyses performed in this work was to estimate the changes in shear wave splitting (SWS) in the reservoir after hydraulic fracturing. SWS was derived after interpreting the PS time horizons. The Montney D and C horizons were interpreted first with the two PS1 and PS2 surveys in the base survey (Phase 1) and then the two monitor surveys (Phase 2 and Phase 3). SWS maps for each survey were created using Equation 20. The difference SWS maps for Unit C and Unit D are shown in **Fig. 6a** and Fig. 6b, respectively. The SWS in Phase 3 is up to 7 times that of SWS in Phase 1. The difference map highlights the changes that have occurred in the target area during flowback. The changes in Montney D appear to be greater than for Montney C - there is also appears to be some indication of fracture communication between Montney C and Montney D.

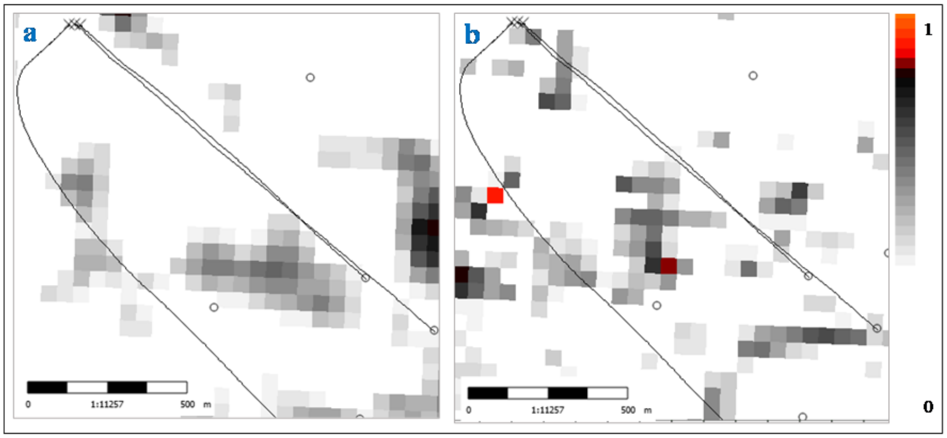

Fig. 6. The difference in shear wave splitting between Phase 3 and Phase 1 for a) Montney C and b) Montney D.

Discussion

In the previous section, it was demonstrated how time-lapse seismic inversion can identify significant changes in the target zone of study area after hydraulic fracturing and flowback. In this section, different time-lapse seismic attributes are compared to determine which ones are best for revealing changes in the reservoir due to these operations. Table 1 summarizes the comparison of the selected time-lapse attributes. As expected from the Riazi et al. (2017) results, Lamé attributes exhibit greater changes compared to V_p and V_s. LambdaRho and MuRho, which are the product of density and Lambda and Mu, respectively, are more sensitive to changes in the reservoir compared to acoustic impedance and shear impedance. Because Lamé attributes have a higher sensitivity to lithology and fluid changes, we recommend the use of these attributes for identifying changes in the reservoir due to hydraulic fracturing and hydrocarbon production.

Table 1. Comparison of time-lapse attribute changes in the target reservoir zone.

Seismic Attributes	Maximum changes (%)
Zp	7.1
Zs	8.5
Vp/Vs	2.5
LambdaRho	22.6
MuRho	19.5
Lambda/Mu	19.5

For confirmation of the time-lapse seismic analyses performed herein, SWS results for Unit D (which were illustrated in Fig. 6) are compared with the microseismic results of Steinhoff (2013) in **Fig. 7**. The SWS difference map of SWS can partially delineate features observed in the microseismic data. Some differences seen in these two maps are due to the fact that the microseismic data are mostly reflecting events associated with hydraulic fracture creation, while time-lapse results are mainly sensitive to changes in the reservoir caused by hydraulic fracturing and subsequent flowback (i.e. changes in effective pressure and fluid saturations in the reservoir). Due to the emphasis on difference results, natural geological features are ignored. As discussed for the results of rock physics modeling, seismic velocities are mostly sensitive to changes in effective pressure. Riazi et al. (2017) also demonstrated that seismic attributes exhibit strong changes with variations in effective pressure.

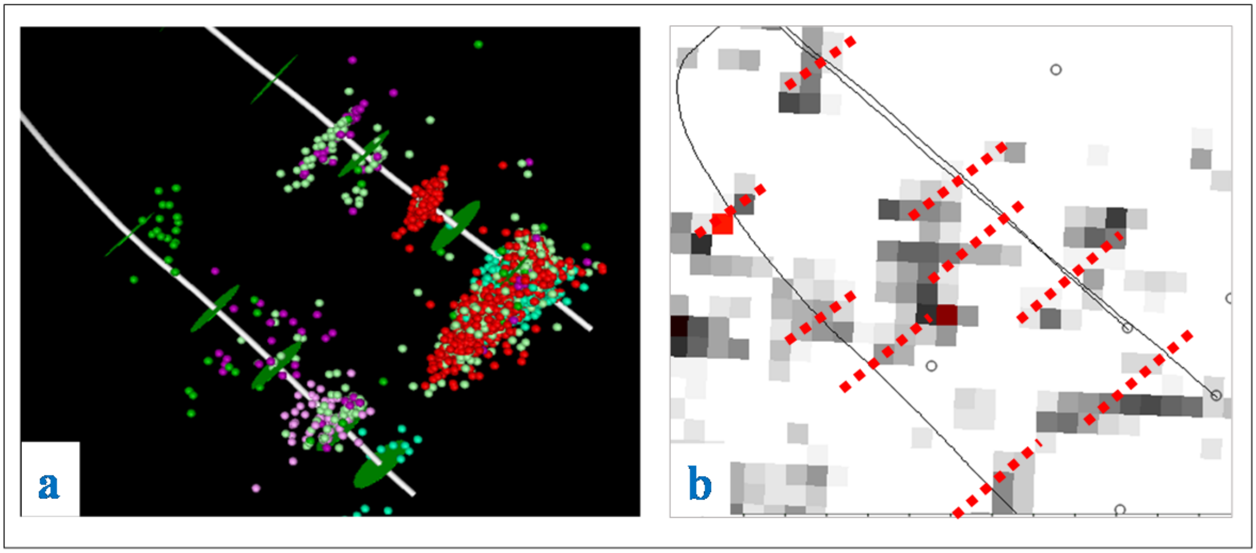

Fig. 7. Comparison of microseismic results (modified from Atkinson 2010) (a) and the difference in SWS obtained for Montney Unit D from time-lapse seismic. Dashed lines show possible trends of hydraulic fractures in (b).

Conclusions

In this work, a comprehensive time-lapse seismic analysis was performed for a tight gas reservoir in western Canada for the purpose of delineating changes in the reservoir after hydraulic fracturing and flowback. The analysis incorporates rock physics modeling, PP time-lapse seismic inversion, and shear wave splitting analyses. The primary conclusions drawn from this study are as follows:

- Rock physics modeling allows the effects of fluid saturation and effective pressure changes in the reservoir during flowback on seismic velocities to be determined. The impact of fluid saturation variation was determined using well log data and through application of Gassmann substitutional modeling. The effective pressure effect was also modeled using velocity-pressure and porosity-pressure relationships obtained from core plug samples of the Montney in another area (Riazi et al. 2017) and for core analyses performed in the study area, respectively. Both saturation and effective pressure affected P- and S-velocities, however the impact of effective pressure is more significant.
- Acoustic impedance, shear impedance, and density volumes were derived for the base (pre-hydraulic fracturing) survey and two monitor surveys (after successive hydraulic fracturing of two adjacent multi-fractured horizontal wells) using a pre-stack seismic inversion algorithm. The difference volumes in these seismic properties aid in monitoring the changes due hydraulic fracturing and flowback in vertical and horizontal directions. One of important benefits of running time-lapse seismic inversion is in quantifying changes in different seismic attributes. Lamé attributes were determined to be more sensitive to hydraulic fracturing and flowback in the study area.
- It is further illustrated that PS seismic data are effective for characterizing fractured regions due to the incorporation of shear wave data along with compressional wave data. Shear wave splitting maps were compared to the results microseismic obtained during hydraulic fracturing – the results of the two analysis methods are in partial agreement but differ somewhat because of the sensitivity of time-lapse seismic to reservoir changes during flowback.

Acknowledgements

The authors would like to thank Repsol Inc. for providing the dataset used in this study. We would particularly like to thank David D’Amico of Repsol for his thoughtful discussion of time-lapse seismic results. Chris Clarkson would like to acknowledge Shell, Encana, and Alberta Innovates Technology Futures for support of his Chair position in Unconventional Gas and Light Oil at the University of Calgary, Department of Geoscience.

Nomenclature

Abbreviations

MFHW	multi-fractured horizontal well
SWS	shear wave splitting
Lambda	lamé parameter
Mu	lamé parameter
LambdaRho	product of Lambda and density
MuRho	product of Mu and density

Field variables

c	stiffness coefficient
D	derivative matrix
G	shear modulus
K	bulk modulus
V_P	P-wave velocity
V_S	shear velocity
R	reflectivity
S	saturation
W	wavelet

Subscripts

sat	in reference to saturated elastic properties
dry	in reference to dry elastic properties
m	in reference to mineral elastic properties
fl	in reference to fluid elastic properties
eff	effective
P	in reference to P-reflectivity
S	in reference to S-reflectivity
D	in reference to density reflectivity
g	in reference to gas
o	in reference to oil
w	in reference to water

Greek variables

γ	second Thomsen parameter
λ	lamé parameter
μ	lamé parameter
ρ	bulk density
θ	angle of incidence

References

Aki, K., and Richards, P.G. 1980. *Quantitative Seismology*. Freeman and Co.

Atkinson, J., 2010. Multicomponent Time-Lapse Monitoring Of Two Hydraulic Fracture Stimulations in an Unconventional Reservoir, Pouce Coupe Field, Canada. M.Sc. thesis, Colorado School of Mines, Golden, Colorado, 119 p.

Clarkson, C. R., and Beierle, J. J. 2011. Integration of Microseismic and other Post-Fracture Surveillance with Production Analysis: A Tight Gas Study. *Journal of Natural Gas Science and Engineering* 3(2): 382-401.

Clarkson, C. R., Jensen, J. L., and Chipperfield, S. 2012a. Unconventional Gas reservoir Evaluation: What Do We Have to Consider? *Journal of Natural Gas Science and Engineering* 8: 9-33.

Clarkson, C. R., Jensen, J. L., Pedersen, P. K., and Freeman, M. 2012b. Innovative Methods for Flow-unit and Pore-Structure Analyses in a Tight siltstone and Shale Gas Reservoir. *AAPG bulletin* 96(2): 355-374.

Clarkson, C. R. et al. 2016. Nanopores to Megafractures: Current Challenges and Methods for Shale Gas Reservoir and Hydraulic Fracture Characterization. *Journal of Natural Gas Science and Engineering* 31: 612-657.

Duenas, C., 2014. Understanding Rock Quality Heterogeneity of Montney Shale Reservoir, Pouce Coupe Field, Alberta, Canada. Colorado School of Mines.

Edwards, D. E., Barclay, J. E., Gibson, D. W., Kvill, G. E., and Halton, E. 1994. *Triassic Strata of the Western Canada Sedimentary Basin. Geological Atlas of the Western Canada Sedimentary Basin*. GD Mossop and I. Shetsen (comps.). Canadian Society of Petroleum Geologists and Alberta Research Council, 257-275.

Fatti, J.L., Smith, G.C., Vail, P.J., Strauss, P.J., and Levitt, P.R. 1994. Detection of Gas in Sandstone Reservoirs using AVO Analysis: a 3D Seismic Case History Using the Geostack Technique. *Geophysics* 59: 1362-1376.

Gassmann, F., 1951. Uber die Elastizitat poroser Medien, Vierteljarhrsschirift der Naturforschenden Gesellschaft in Zurich, Vol. 96, p. 1-23.

Goodway, B., Perez, M., Varsek, J., and Abaco, C. 2010. Seismic Petrophysics and Isotropic-Anisotropic AVO Methods for Unconventional Gas Exploration. *The Leading Edge* 29(12): 1500-1508.

Hampson, D.P., Russell, B.H., and Bankhead, B. 2005. Simultaneous Inversion of Pre-Stack Seismic Data. Ann. Mtg. Abstracts, SEG, p. 1633-1637.

Kendall, D., 1999. Sedimentology and Stratigraphy of the Lower Triassic Montney Formation, Peace River Basin, Subsurface of Northwestern Alberta. M.Sc. thesis, University of Calgary.

Lumley, D. E., 2001. Time-lapse Seismic Reservoir Monitoring. *Geophysics* 66(1): 50-53.

Mirzayev, M., Riazi, N., Cronkwright, D., Jensen, J. L., and Pedersen, P. K. 2017. Determining Well-to-Well Connectivity using a Modified Capacitance Model, Seismic, and Geology for a Bakken Waterflood. *Journal of Petroleum Science and Engineering* 152: 611-627.

Riazi, N., Clarkson, C. R., Ghanizadeh, A., Vahedian, A., Aquino, S., and Wood, J. M. 2017. Determination of Elastic Properties of Tight Rocks from Ultrasonic Measurements: Examples from the Montney Formation (Alberta, Canada). *Fuel* 196: 442-457.

Riazi, N., Lines, L., and Russell, B. 2015. Monitoring Heavy Oil Recovery by Time-Lapse EEI Inversion. *Journal of Seismic Exploration*, 24(4): 343-364.

Riazi, N., and Clarkson, C. R. 2016. The Importance of Seismic Attributes in Reservoir Characterization and Inter-Well Connectivity Studies of Tight Oil Reservoirs, Geoconvention, March 2016.

Steinhoff, C., 2013. Multicomponent Seismic Monitoring of the Effective Stimulated Volume Associated with Hydraulic Fracture Stimulations in a Shale Reservoir, Pouce Coupe Field, Alberta, Canada. Colorado School of Mines.

Teanby, N., Kendall, J. M., Jones, R. H., and Barkved, O. 2004. Stress-Induced Temporal Variations in Seismic Anisotropy Observed in Microseismic Data. *Geophysical Journal International* 156(3): 459-466.

Thomsen, L., 1986. Weak Elastic Anisotropy. *Geophysics* 51(10): 1954-1966.

Verdon, J. P., and Kendall, J. 2011. Detection of Multiple Fracture Sets using Observations of Shear-Wave Splitting in Microseismic Data. *Geophysical Prospec*ting 59(4): 593-608.